Probability of Error of OFDM Systems with Carrier Frequency Offset in Frequency-Selective Fading Channels

L. Rugini, P. Banelli, S. Cacopardi
Dipartimento di Ingegneria Elettronica e dell'Informazione (D.I.E.I.)
University of Perugia
Perugia, Italy

***Abstract*—We present an analytical approach to evaluate the error probability of orthogonal frequency-division multiplexing (OFDM) systems subject to carrier frequency offset (CFO) in frequency-selective channels, characterized by Rayleigh or Rician fading. By exploiting the Gaussian approximation of the intercarrier interference (ICI), we show that the bit-error rate (BER) for quadrature amplitude modulation (QAM) can be expressed by the sum of few integrals, whose number depends on the constellation size. Each integral can be evaluated numerically, or, in Rayleigh fading, by using a series expansion that involves generalized hypergeometric functions. Simulation results illustrate that the theoretical analysis is quite accurate, especially for Rayleigh channels.**

Keywords-OFDM; carrier frequency offset; frequency-selective fading channels; BER

I. INTRODUCTION

Orthogonal frequency-division multiplexing (OFDM) is a technique widely used for wireless applications [1]. Due to its multicarrier feature, OFDM systems are more sensitive than single-carrier systems to frequency synchronization errors [2]. Indeed the carrier frequency offset (CFO), which models the mismatch between the transmitter and receiver oscillators (or represents the Doppler shift introduced by the time-varying channel), gives rise to intercarrier interference (ICI), thereby destroying the orthogonality of the OFDM data.

In linearly modulated OFDM systems, the performance degradation caused by the CFO is often evaluated in terms of signal-to-noise ratio (SNR) loss [2]-[4]. The degradation due to the CFO is also analyzed in [5]-[7] in terms of bit-error rate (BER) or symbol-error rate (SER). Although the BER characterizes the performance degradation more accurately with respect to the SNR loss, [5], [6], and [7] consider the CFO effects only in additive white Gaussian noise (AWGN) channels, whereas OFDM systems are usually designed to cope with frequency-selective fading [1].

In this paper, we present a BER analysis when the CFO impairs an OFDM system in frequency-selective Rician fading channels. By exploiting the Gaussian approximation of the ICI, we show that the BER for quadrature amplitude modulation (QAM) can be obtained as the sum of few integrals, whose number depends on the constellation size. Each integral can be computed by numerical techniques, or, in Rayleigh fading, replaced by a series expansion that involves generalized hypergeometric functions. Simulation results are used in order to validate the theoretical analysis.

This work was partially supported by the Italian Minister of University and Research under the project "OFDM Systems with Applications to WLAN Networks."

II. OFDM SYSTEM MODEL

An OFDM system with N subcarriers and a cyclic prefix of length L is considered. Using a notation similar to [8], the lth transmitted block can be expressed as

$$\mathbf{u}[l] = \mathbf{T}_{\mathrm{CP}}\mathbf{F}^{H}\mathbf{s}[l], \tag{1}$$

where $\mathbf{u}[l]$ is a column vector of dimension $P = N + L$, $\mathbf{F}$ is the $N \times N$ unitary fast Fourier transform (FFT) matrix, defined by $[\mathbf{F}]_{m,n} = N^{-1/2}\exp(-j2\pi(m-1)(n-1)/N)$, $\mathbf{s}[l]$ is the $N \times 1$ vector that contains the data symbols, and $\mathbf{T}_{\mathrm{CP}} = [\mathbf{I}_{\mathrm{CP}}^{T}\ \mathbf{I}_{N}^{T}]^{T}$ is the $P \times N$ matrix that inserts the cyclic prefix, where $\mathbf{I}_{\mathrm{CP}}$ contains the last L rows of the identity matrix $\mathbf{I}_{N}$. The data symbols, assumed to be independent and identically distributed with power $\sigma_{\mathrm{S}}^{2} = 1$, are modulated using M-ary square QAM.

After the parallel-to-serial conversion, the stream $u[lP+n] = [\mathbf{u}[l]]_{n}$, where $[\mathbf{u}[l]]_{n}$ is the nth element of $\mathbf{u}[l]$, is transmitted through a multipath channel, whose discrete-time equivalent impulse response is

$$h[i] = \sum_{q=1}^{Q} \zeta_{q} R_{\psi}(iT_{\mathrm{S}} - \tau_{q}), \tag{2}$$

where Q is the number of paths of the channel, ζ_{q} and τ_{q} are the complex amplitude and the propagation delay, respectively, of the qth path, $R_{\psi}(\tau)$ is the triangular autocorrelation function of the rectangular pulse shaping waveform $\psi(t)$, and $T_{\mathrm{S}} = T/N$ is the sampling period, being $\Delta_{f} = 1/T$ the subcarrier spacing. Throughout the paper, we assume that the channel amplitudes $\{\zeta_{q}\}$ are Gaussian distributed, giving rise to Rayleigh or Rician fading, and that the maximum delay spread $\tau_{\max} = \max\{\tau_{q}\}$ is smaller than the cyclic prefix duration $\tau_{\mathrm{CP}} = LT_{\mathrm{S}}$, i.e., $h[i] = 0$ for $i > L$.

At the receiver side, the samples obtained after matched filtering can be expressed as [9]

$$x[p] = e^{j2\pi f_0 pT_S} \sum_{i=0}^{L} h[i]u[p-i] + w[p], \quad (3)$$

where f_0 is the CFO, and $w[p]$ represents the AWGN. Assuming that the timing information is available at the receiver, the P received samples relative to the lth OFDM block are grouped in the vector $\mathbf{x}[l]$, thus obtaining [9]

$$\mathbf{x}[l] = e^{j2\pi\varepsilon lP/N}\tilde{\mathbf{D}}(\mathbf{H}_0\mathbf{u}[l] + \mathbf{H}_1\mathbf{u}[l-1]) + \mathbf{w}[l], \quad (4)$$

where $[\mathbf{x}[l]]_n = x[lP+n]$, $\varepsilon = f_0 T$ is the normalized CFO, $\tilde{\mathbf{D}}$ is a $P\times P$ diagonal matrix defined by $[\tilde{\mathbf{D}}]_{n,n} = \exp(j2\pi\varepsilon(n-1)/N)$, and $\mathbf{H}_0$ and $\mathbf{H}_1$ are $P\times P$ Toeplitz matrices defined by $[\mathbf{H}_0]_{m,n} = h[m-n]$ and $[\mathbf{H}_1]_{m,n} = h[m-n+P]$, respectively [8]. By applying the matrix $\mathbf{R}_{CP} = [\mathbf{0}_{N\times L}\ \mathbf{I}_N]$ to $\mathbf{x}[l]$ in (4), the cyclic prefix (and hence the interblock interference) is eliminated, thus obtaining, by (1), the $N\times 1$ vector [9]

$$\mathbf{y}[l] = \mathbf{R}_{CP}\mathbf{x}[l] = e^{j2\pi\varepsilon(lP+L)/N}\mathbf{D}\mathbf{H}\mathbf{F}^H\mathbf{s}[l] + \mathbf{v}[l], \quad (5)$$

where $\mathbf{D}$ is an $N\times N$ diagonal matrix expressed by $[\mathbf{D}]_{n,n} = \exp(j2\pi\varepsilon(n-1)/N)$, and $\mathbf{H} = \mathbf{R}_{CP}\mathbf{H}_0\mathbf{T}_{CP}$ is the circulant channel matrix expressed by $[\mathbf{H}]_{m,n} = h[(m-n)_{\mathrm{mod}\,N}]$. By applying the FFT at the receiver, we obtain $\mathbf{z}[l] = \mathbf{F}\mathbf{y}[l]$, which by (5) can be rearranged as

$$\mathbf{z}[l] = e^{j2\pi\varepsilon(lP+L)/N}\mathbf{\Phi}\mathbf{\Lambda}\mathbf{s}[l] + \mathbf{n}[l], \quad (6)$$

where $\mathbf{\Phi} = \mathbf{F}\mathbf{D}\mathbf{F}^H$ is the circulant matrix that produces the ICI, $\mathbf{\Lambda} = \mathbf{F}\mathbf{H}\mathbf{F}^H$ is the diagonal matrix containing the frequency-domain channel, with elements expressed by

$$\lambda_n = [\mathbf{\Lambda}]_{n,n} = \sum_{i=0}^{L} h[i]e^{-j2\pi i(n-1)/N}, \quad (7)$$

and $\mathbf{n}[l] = \mathbf{F}\mathbf{v}[l] = \mathbf{F}\mathbf{R}_{CP}\mathbf{w}[l]$ represents the AWGN. From the above definitions, it is straightforward to verify that

$$[\mathbf{\Phi}]_{m,n} = \frac{\sin(\pi((n-m)_{\mathrm{mod}\,N}+\varepsilon))}{N\sin(\pi((n-m)_{\mathrm{mod}\,N}+\varepsilon)/N)} e^{j\pi\frac{N-1}{N}((n-m)_{\mathrm{mod}\,N}+\varepsilon)}, \quad (8)$$

and that $\boldsymbol{\lambda} = \sqrt{N}\,\mathbf{F}\mathbf{h}$, being $\mathbf{h} = [h[0],...,h[N-1]]^T$ and $\boldsymbol{\lambda} = [\lambda_1,...,\lambda_n]^T$ the channel vectors in the time domain and frequency domain, respectively.

Assuming perfect channel state information at the receiver side, after compensating for the phase-shift term $\varphi[l] = \exp(j2\pi\varepsilon(lP+L)/N)\exp(j\pi\varepsilon(N-1)/N)$ that is common to all the subcarriers, and after performing the zero-forcing equalization, from (6) we obtain

$$\mathbf{z}_{EQ}[l] = \varphi[l]^*\mathbf{\Lambda}^{-1}\mathbf{z}[l] = \mathbf{\Lambda}^{-1}\mathbf{M}\mathbf{\Lambda}\mathbf{s}[l] + \mathbf{n}_{EQ}[l], \quad (9)$$

where $\mathbf{M} = \exp(-j\pi\varepsilon(N-1)/N)\mathbf{\Phi}$ contains the CFO, and $\mathbf{n}_{EQ}[l] = \varphi[l]^*\mathbf{\Lambda}^{-1}\mathbf{n}[l]$. The decision over $\mathbf{z}_{EQ}[l]$ is successively done according to the proper constellation size M.

III. BER OF OFDM WITH CFO IN FADING CHANNELS

In order to evaluate the error probability, without loss of generality, we focus on the signal received on the first subcarrier, dropping the block index l for the sake of simplicity. We consider a scaled version of the decision variable, obtained from (9), as expressed by

$$z_1 = \lambda_1 z_{EQ,1} = m_1\lambda_1 s_1 + \sum_{n=2}^{N} m_n\lambda_n s_n + n_1, \quad (10)$$

where $z_{EQ,1} = [\mathbf{z}_{EQ}[l]]_1$, $s_n = [\mathbf{s}[l]]_n$, $n_1 = \varphi[l]^*[\mathbf{n}[l]]_1$, and

$$m_n = [\mathbf{M}]_{1,n} = \frac{\sin(\pi(n-1+\varepsilon))}{N\sin(\pi(n-1+\varepsilon)/N)} e^{j\pi\frac{N-1}{N}(n-1)} \quad (11)$$

represents the ICI coefficient when $n = 2,...,N$, and the attenuation factor of the useful signal when $n = 1$.

One possible approach to obtain the BER (or equivalently the SER) consists of two steps. In the first one, we have to calculate the conditional bit-error probability $P_{BE}(\mathbf{s},\boldsymbol{\lambda})$ as a function of the symbols in $\mathbf{s} = [s_1,...,s_n]^T$ and of the channel amplitudes in $\boldsymbol{\lambda} = [\lambda_1,...,\lambda_n]^T$. In the second step, $P_{BE}(\mathbf{s},\boldsymbol{\lambda})$ has to be integrated over the joint probability density function (pdf) $f_{S,\Lambda}(\mathbf{s},\boldsymbol{\lambda}) = f_S(\mathbf{s})f_\Lambda(\boldsymbol{\lambda})$ of the symbols and the channel amplitudes, as expressed by

$$\mathrm{BER} = \int_{\mathbf{s},\boldsymbol{\lambda}} P_{BE}(\mathbf{s},\boldsymbol{\lambda})f_S(\mathbf{s})f_\Lambda(\boldsymbol{\lambda})d\mathbf{s}d\boldsymbol{\lambda}. \quad (12)$$

The main difficulty in evaluating (12) is due to the presence of the N-dimensional pdf $f_\Lambda(\boldsymbol{\lambda})$. Indeed, when dealing with multidimensional integrations, it would be easier to evaluate many separated single-variable integrals, one at a time. However, from (7), it is evident that the N variables in $\boldsymbol{\lambda}$ are correlated with one another, because the frequency-domain channel is obtained by combining at most $L+1$ random variables. Therefore, $f_\Lambda(\boldsymbol{\lambda})$ cannot be expressed as a product of N separate one-dimensional functions. In order to overcome this problem, we bypass the multidimensional integration by using the equality given by $f_\Lambda(\boldsymbol{\lambda}) = f_{\bar{\Lambda}|\lambda_1}(\bar{\boldsymbol{\lambda}}|\lambda_1)f_{\lambda_1}(\lambda_1)$, where $f_{\bar{\Lambda}|\lambda_1}(\bar{\boldsymbol{\lambda}}|\lambda_1)$ is the conditional pdf of $\bar{\boldsymbol{\lambda}} = [\lambda_2,...,\lambda_n]^T$ given λ_1, and $f_{\lambda_1}(\lambda_1)$ is the pdf of λ_1. Therefore, (12) becomes

$$\mathrm{BER} = \int_{\lambda_1} P_{BE}(\lambda_1)f_{\lambda_1}(\lambda_1)d\lambda_1, \quad (13)$$

$$P_{BE}(\lambda_1) = \int_{\mathbf{s},\bar{\boldsymbol{\lambda}}} P_{BE}(\mathbf{s},\boldsymbol{\lambda})f_{\bar{\Lambda}|\lambda_1}(\bar{\boldsymbol{\lambda}}|\lambda_1)f_S(\mathbf{s})d\mathbf{s}d\bar{\boldsymbol{\lambda}}. \quad (14)$$

In the following, we show that it is possible to approximate $P_{BE}(\lambda_1)$ without solving the integral in (14). Hence, by (13), the BER is given by an integral over a single complex variable.

A. BER Evaluation in Rayleigh Fading Channels

When the channel experiences Rayleigh fading, the channel taps $\{h[i]\}$, and hence the quantities $\{\lambda_n\}$ in (7), are zero-mean complex Gaussian random variables. In this case, the conditional pdf $f_{\bar{\Lambda}|\lambda_1}(\bar{\boldsymbol{\lambda}}|\lambda_1)$ is an $(N-1)$-dimensional Gaussian with mean $\boldsymbol{\eta}_{\bar{\lambda}|\lambda_1}$ and covariance $\mathbf{C}_{\bar{\lambda}|\lambda_1}$ expressed by [10]

$$\boldsymbol{\eta}_{\bar{\lambda}|\lambda_1} = \lambda_1 c_{\lambda_1\lambda_1}^{-1}\mathbf{c}_{\bar{\lambda}\lambda_1}, \quad (15)$$

$$\mathbf{C}_{\bar{\lambda}|\lambda_1} = \mathbf{C}_{\bar{\lambda}\bar{\lambda}} - c_{\lambda_1\lambda_1}^{-1}\mathbf{c}_{\bar{\lambda}\lambda_1}\mathbf{c}_{\bar{\lambda}\lambda_1}^H, \quad (16)$$

where

$$\mathbf{C}_{\lambda\lambda} = E\{\boldsymbol{\lambda}\boldsymbol{\lambda}^H\} = \begin{bmatrix} c_{\lambda_1\lambda_1} & \mathbf{c}_{\bar{\lambda}\lambda_1}^H \\ \mathbf{c}_{\bar{\lambda}\lambda_1} & \mathbf{C}_{\bar{\lambda}\bar{\lambda}} \end{bmatrix} \quad (17)$$

is the covariance matrix of the frequency-domain channel, related to the covariance matrix $\mathbf{C}_{\mathbf{hh}} = E\{\mathbf{h}\mathbf{h}^H\}$ of the time-domain channel by $\mathbf{C}_{\lambda\lambda} = N\mathbf{F}\mathbf{C}_{\mathbf{hh}}\mathbf{F}^H$. After forming the conditional random variable $t_1 = z_1|\lambda_1$, from (10) we obtain

$$t_1 = m_1\lambda_1 s_1 + \sum_{n=2}^{N} m_n k_n s_n + n_1, \quad (18)$$

where the conditional random variable $k_n = \lambda_n \mid \lambda_1$ is Gaussian with mean value obtained by (15) as $\eta_n = E\{k_n\} = \lambda_1 c^{-1}_{\lambda_1\lambda_1}[\mathbf{c}_{\bar{\lambda}\lambda_1}]_{n-1}$. Consequently, by splitting $k_n = \eta_n + \kappa_n$, (18) becomes

$$t_1 = m_1\lambda_1 s_1 + \alpha_1\lambda_1 + \beta_1 + n_1, \tag{19}$$

$$\alpha_1 = c^{-1}_{\lambda_1\lambda_1}\sum_{n=2}^{N} m_n[\mathbf{c}_{\bar{\lambda}\lambda_1}]_{n-1}s_n, \qquad \beta_1 = \sum_{n=2}^{N} m_n\kappa_n s_n. \tag{20}$$

From (19)-(20), it is evident that the ICI consists of two parts. The first part, $\alpha_1\lambda_1$, is proportional to the channel amplitude λ_1 of the useful signal. Hence $\alpha_1\lambda_1$ represents the ICI part that fades *simultaneously* with the useful signal. Its power can be expressed by $|\lambda_1|^2\sigma^2_{\mathrm{ICI},\alpha}$, where

$$\sigma^2_{\mathrm{ICI},\alpha} = |c^{-1}_{\lambda_1\lambda_1}|^2 \sum_{n=2}^{N} |m_n[\mathbf{c}_{\bar{\lambda}\lambda_1}]_{n-1}|^2. \tag{21}$$

On the other hand, the second part β_1 has a power that is *independent* of λ_1, as expressed by

$$\sigma^2_{\mathrm{ICI},\beta} = \sum_{n=2}^{N} |m_n|^2 [\mathbf{C}_{\bar{\lambda}|\lambda_1}]_{n-1,n-1}. \tag{22}$$

Since $\alpha_1\lambda_1$ and β_1 are uncorrelated, the signal-to-interference plus noise ratio (SINR) conditioned on λ_1 can be expressed as

$$\gamma = \frac{|\lambda_1|^2 |m_1|^2}{|\lambda_1|^2\sigma^2_{\mathrm{ICI},\alpha} + \sigma^2_{\mathrm{ICI},\beta} + \sigma^2_{\mathrm{AWGN}}}, \tag{23}$$

where $\sigma^2_{\mathrm{AWGN}} = E\{|n_1|^2\}$.

As far as the statistical characterization of the ICI is concerned, we observe that α_1 in (20), apart for the scalar $c^{-1}_{\lambda_1\lambda_1}$, is obtained by the sum of the independent data symbols $\{s_n\}_{n=2}^N$, each one weighted by the coefficient $m_n[\mathbf{c}_{\bar{\lambda}\lambda_1}]_{n-1}$. As a consequence, since practical OFDM systems have a high number N of subcarriers [1], the central limit theorem allows to approximate α_1 as a Gaussian variable with zero mean and variance $\sigma^2_{\mathrm{ICI},\alpha}$ expressed by (21). Likewise, β_1 in (20) is a linear combination of the random variables $\{\kappa_n s_n\}_{n=2}^N$. Since the coefficients $\{\kappa_n\}_{n=2}^N$ are jointly Gaussian, the pdf of $\kappa_n s_n$ is a weighted sum of Gaussian functions. Therefore, for quaternary phase-shift keying (QPSK), i.e., 4-QAM, the pdf of β_1 is Gaussian, while, for higher-order QAM, it is approximately Gaussian by the central limit theorem. In all cases, the mean of β_1 is zero, and its variance is expressed by (22). We underline that the Gaussian approximation of the CFO-induced ICI has been already exploited for AWGN channels [7]. In Section IV, we will check its accuracy in multipath scenarios.

As a consequence of the Gaussian approximation, for QAM modulations with Gray coding, it is straightforward to obtain the conditional BER $P_{\mathrm{BE}}(\lambda_1)$ as a function of the conditional SINR. For example, the conditional BER for QPSK is expressed by $P_{\mathrm{BE}}(\lambda_1) = Q(\gamma^{1/2})$, while for 16-QAM it can be expressed by [11]

$$P_{\mathrm{BE}}(\lambda_1) = \frac{3}{4}Q\left(\sqrt{\frac{1}{5}\gamma}\right) + \frac{1}{2}Q\left(\sqrt{\frac{9}{5}\gamma}\right) - \frac{1}{4}Q\left(\sqrt{5\gamma}\right). \tag{24}$$

In this case the BER, obtained by inserting (23)-(24) in (13), is the sum of three integrals. In the general M-QAM case, the number of such integrals is equal to $\sqrt{M}-1$ [11].

By (23)-(24), it is evident that $P_{\mathrm{BE}}(\lambda_1)$ depends only on $|\lambda_1|$, and therefore the integration variable can be real. Moreover, since $|\lambda_1|$ has a Rayleigh pdf, each integral can be replaced by a series expansion of ${}_2F_0$-type generalized hypergeometric functions [12]. For QPSK, the final results is

$$\mathrm{BER} = \frac{1}{2} - \frac{\sqrt{2}\mu}{4} e^{-\frac{\mu^2}{2\nu^2}} \sum_{k=0}^{+\infty} \frac{\mu^{2k}}{k!2^k\nu^{2k}}\, {}_2F_0\left(k+\frac{3}{2}, \frac{1}{2};;-\nu^2\right), \tag{25}$$

$$\mu^2 = \frac{c_{\lambda_1\lambda_1}|m_1|^2}{\sigma^2_{\mathrm{ICI},\beta} + \sigma^2_{\mathrm{AWGN}}}, \quad \nu^2 = \frac{c_{\lambda_1\lambda_1}\sigma^2_{\mathrm{ICI},\alpha}}{\sigma^2_{\mathrm{ICI},\beta} + \sigma^2_{\mathrm{AWGN}}}. \tag{26}$$

A simple and accurate criterion for truncating the summation in (25) can be found in [12].

B. BER Evaluation in Rician Fading Channels

In Rician fading channels, we assume that a single line-of-sight (LOS) is present, i.e., that $h[0]$ in (2) is characterized by a non-zero mean value, and we use the same approach adopted in the Rayleigh case. From [10], the conditional pdf $f_{\bar{\Lambda}|\lambda_1}(\bar{\boldsymbol{\lambda}}\,|\,\lambda_1)$ is an $(N-1)$-dimensional Gaussian with covariance again expressed by (16), and mean value expressed by

$$\boldsymbol{\eta}_{\bar{\lambda}|\lambda_1} = \lambda_{\mathrm{LOS}}\mathbf{1}_{N-1} + \lambda_{1,\mathrm{NLOS}}c^{-1}_{\lambda_1\lambda_1}\mathbf{c}_{\bar{\lambda}\lambda_1}, \tag{27}$$

where $\lambda_{\mathrm{LOS}} = E\{\lambda_1\}$, $\lambda_{1,\mathrm{NLOS}} = \lambda_1 - \lambda_{\mathrm{LOS}}$, and $\mathbf{1}_{N-1}$ is the $(N-1)$-dimensional all-one vector. By setting $t_1 = z_1 \mid \lambda_1$, from (10) we obtain an expression equivalent to (18), where the conditional random variable $k_n = \lambda_n \mid \lambda_1$ is Gaussian with mean value $\eta_n = \lambda_{\mathrm{LOS}} + \lambda_{1,\mathrm{NLOS}}c^{-1}_{\lambda_1\lambda_1}[\mathbf{c}_{\bar{\lambda}\lambda_1}]_{n-1}$. In this case, t_1 can be expressed as

$$t_1 = m_1\lambda_{\mathrm{LOS}}s_1 + m_1\lambda_{1,\mathrm{NLOS}}s_1 + \alpha_1\lambda_{1,\mathrm{NLOS}} + \chi_1 + \beta_1 + n_1, \tag{28}$$

where α_1 and β_1 are defined in (20), and

$$\chi_1 = \lambda_{\mathrm{LOS}}\sum_{n=2}^{N} m_n s_n. \tag{29}$$

By exploiting the Gaussian approximation, for Gray-mapped QAM, the conditional BER $P_{\mathrm{BE}}(\lambda_1)$ is expressed as the sum of Q-type functions like the one in (24), with SINR given by

$$\gamma = \frac{|\lambda_1|^2|m_1|^2}{|\lambda_{1,\mathrm{NLOS}}|^2\sigma^2_{\mathrm{ICI},\alpha} + 2\rho_{\mathrm{ICI},\alpha,\chi} + \sigma^2_{\mathrm{ICI},\chi} + \sigma^2_{\mathrm{ICI},\beta} + \sigma^2_{\mathrm{AWGN}}}, \tag{30}$$

$$\sigma^2_{\mathrm{ICI},\chi} = |\lambda_{\mathrm{LOS}}|^2 \sum_{n=2}^{N} |m_n|^2, \tag{31}$$

$$\rho_{\mathrm{ICI},\alpha,\chi} = \sum_{n=2}^{N} |m_n|^2\, \mathrm{Re}[\lambda_{1,\mathrm{NLOS}}\lambda^*_{\mathrm{LOS}}c^{-1}_{\lambda_1\lambda_1}[\mathbf{c}_{\bar{\lambda}\lambda_1}]_{n-1}]. \tag{32}$$

The final BER is then obtained by numerical integration of the integral expressed by (13).

C. BER Evaluation in the Presence of Guard Bands

So far, we have assumed that all the N subcarriers are active, although any practical OFDM system contains some virtual (or null) subcarriers used as guard frequency bands [1]. However, it is easy to extend the BER analysis in order to take into account the presence of V virtual subcarriers, because a virtual subcarrier does not contribute to the ICI. As an example, assume that the null subcarriers are the ones with $n \in \{N-V+1, N-V+2, ..., N\}$. The only modification to the previous analysis is that $s_n = 0$ for these subcarriers. Therefore, the BER analysis remains still valid, provided that (21), (22), (31), and (32) are truncated up to $n = N-V$. Obviously,

in this case the BER is not the same for all the active subcarriers, because, when the subcarriers are close to the guard bands, the ICI power is smaller.

IV. Simulation Results

In this section, we present some simulation results in order to validate the Gaussian approximation applied in the theoretical analysis. We consider an OFDM system with cyclic prefix of length $L = 16$, and $N = 64$ subcarriers, spaced with one another by $\Delta_f = 1/T = 312.5$ kHz. We use the channel models B and D of the IEEE 802.11a wireless local area network (WLAN) standard [13]. In the models B and D, each tap suffers independent Rayleigh and Rician fading, respectively, with an exponentially decaying power delay profile, and an rms delay spread equal to 100 ns and 140 ns, respectively.

Fig. 1 shows the BER performance of QPSK as a function of $E_b / N_0 = c_{\lambda_1 \lambda_1} / (\sigma^2_{\text{AWGN}} \log_2 M)$ in the Rayleigh channel B. It is evident that the theoretical analysis exactly predicts the simulated BER for different values of the normalized CFO ε. Such a good agreement clearly indicates that, differently from the AWGN case [7], in frequency-selective scenarios the Gaussian approximation of the ICI leads to accurate results. The motivation of this accuracy is explained in the following. When approximating the sum of many variables by a single Gaussian variable, the approximation gets worse at the tail of the Gaussian, and consequently the approximated BER is not sufficiently accurate when the true BER is small. The mismatch between the approximated and the exact BER happens not only in AWGN channels, but also for the conditional BER $P_{\text{BE}}(\lambda_1)$ in our scenario. However, in fading channels, the BER is obtained by averaging $P_{\text{BE}}(\lambda_1)$ over the pdf of λ_1, and hence it is practically imposed by the values of $P_{\text{BE}}(\lambda_1)$ that correspond to small values of $|\lambda_1|$ [14]. For these values, the Gaussian approximation is very good, because $P_{\text{BE}}(\lambda_1)$ is high, and therefore the obtained BER exactly matches with the true BER. This behavior is confirmed by the results of Figs. 2-3, which show the BER for 16-QAM, and the BER of QPSK as a function of the normalized CFO ε, respectively. Figs. 1-2 report also the BER performance obtained using the ICI approximation proposed in [15], which mainly deals with the effect of the channel estimation errors. Although [15] approximates all the ICI as a zero-mean Gaussian random variable with power independent of the fading gain, (19) shows that part of the ICI is proportional to the fading gain λ_1. Therefore, when $|\lambda_1|$ is low (high), the ICI power is smaller (larger) than the one assumed in [15]. Since most of the errors occur when $|\lambda_1|$ is low, it turns out that in [15] the degradation due to the ICI is overestimated, as confirmed by the BER floors in Figs. 1-2.

Fig. 4 exhibits the BER of the best subcarrier when only $N_{\text{A}} = N - V = 52$ out of $N = 64$ subcarriers are active [13], using QPSK and channel B. Although the ICI is generated by a smaller number of subcarriers, the Gaussian approximation is very accurate in this context too. Figs. 5-6 illustrate the BER performance in channel D with Rician factor $K = 10$, for QPSK and 16-QAM, respectively. In such a scenario, for high values of E_b / N_0, the theoretical BER, obtained by Monte Carlo integration techniques, is less accurate. The reason of this inaccuracy is the high Rician factor K, which produces a high value of λ_{LOS}. Consequently, the term χ_1 in (29) is the dominant one among the ICI terms. Since χ_1 is similar to the ICI term in AWGN channels, we expect that the theoretical BER overestimates the true BER, as in AWGN [7]. Anyway, as shown in Figs. 5-6, this mismatch is very small.

Finally, we want to point out that the Gaussian approximation can be successfully applied not only in WLAN scenarios, but also in broadcasting environments, where thousands of active subcarriers are usually employed [1].

V. Conclusions

We have proposed a theoretical approach that allows to predict the BER of OFDM systems impaired by CFO in multipath Rayleigh (or Rician) fading channels. Simulation results in WLAN scenarios have shown that the proposed approach is characterized by a good level of accuracy. Further studies could also consider the presence of nonlinear distortions [16], channel estimation errors [15], and channel coding.

References

[1] R. van Nee and R. Prasad, OFDM for Wireless Multimedia Communications, Artech House, 2000.

[2] T. Pollet, M. van Bladel, and M. Moeneclaey, "BER sensitivity of OFDM systems to carrier frequency offset and Wiener phase noise," IEEE Trans. Commun., vol. 43, pp. 191-193, Feb./Mar./Apr. 1995.

[3] P. H. Moose, "A technique for orthogonal frequency division multiplexing frequency offset correction," IEEE Trans. Commun., vol. 42, pp. 2908-2914, Oct. 1994.

[4] B. Stantchev and G. Fettweis, "Time-variant distortions in OFDM," IEEE Commun. Lett., vol. 4, pp. 312-314, Sept. 2000.

[5] K. Sathananthan and C. Tellambura, "Probability of error calculation of OFDM systems with frequency offset," IEEE Trans. Commun., vol. 49, pp. 1884-1888, Nov. 2001.

[6] Y. Zhao and S. G. Häggman, "BER analysis of OFDM communication systems with intercarrier interference," in Proc. IEEE Int. Conf. Communication Technology, Beijing, China, Oct. 1998.

[7] T. Keller and L. Hanzo, "Adaptive multicarrier modulation: a convenient framework for time-frequency processing in wireless communications," IEEE Proc., vol. 88, pp. 611-640, May 2000.

[8] Z. Wang and G. B. Giannakis, "Wireless multicarrier communications: where Fourier meets Shannon," IEEE Signal Processing Mag., vol. 17, pp. 29-48, May 2000.

[9] X. Ma, C. Tepedelenlioğlu, G. B. Giannakis, and S. Barbarossa, "Non-data-aided carrier offset estimators for OFDM with null subcarriers: identifiability, algorithms, and performance," IEEE J. Select. Areas Commun., vol. 19, pp. 2504-2515, Dec. 2001.

[10] S. M. Kay, Fundamentals of Statistical Signal Processing: Estimation Theory, vol. 1, Prentice-Hall, 1993.

[11] K. Cho and D. Yoon, "On the general BER expression of one- and two-dimensional amplitude modulations," IEEE Trans. Commun., vol. 50, pp. 1074-1080, July 2002.

[12] L. Rugini and P. Banelli, "Symbol error probability of linearly modulated signals affected by Gaussian interference in Rayleigh fading channels," Tech. Rep. RT-005-03, Dept. Elect. Inform. Eng., Perugia, Italy, Dec. 2003. Available: http://www.diei.unipg.it/rt/DIEI_RT.htm

[13] A. Doufexi et al., "A comparison of the HIPERLAN/2 and IEEE 802.11a wireless LAN standards," IEEE Commun. Mag., vol. 40, pp. 172-180, May 2002.

[14] Z. Wang and G. B. Giannakis, "A simple and general parameterization quantifying performance in fading channels," IEEE Trans. Commun., vol. 51, pp. 1389-1398, Aug. 2003.

[15] H. Cheon and D. Hong, "Effect of channel estimation error in OFDM-based WLAN," IEEE Commun. Lett., vol.6, pp. 190-192, May 2002.

[16] P. Banelli and S. Cacopardi, "Theoretical analysis and performance of OFDM signals in nonlinear AWGN channels," IEEE Trans. Commun., vol. 48, pp. 430-441, Mar. 2000.

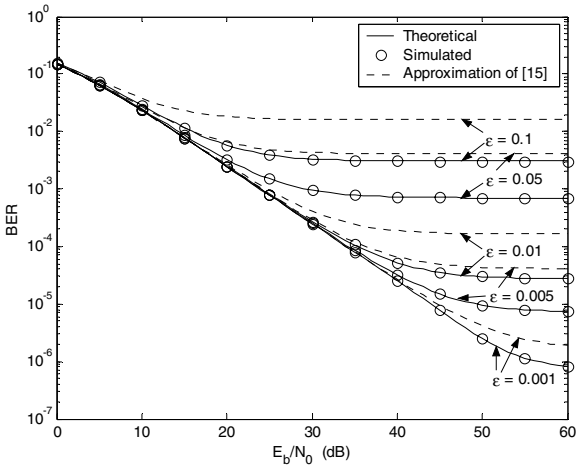

Figure 1. BER of QPSK in the Rayleigh channel B.

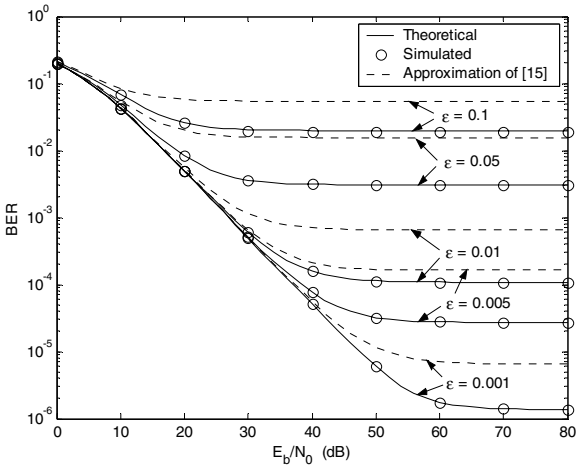

Figure 2. BER of 16-QAM in the Rayleigh channel B.

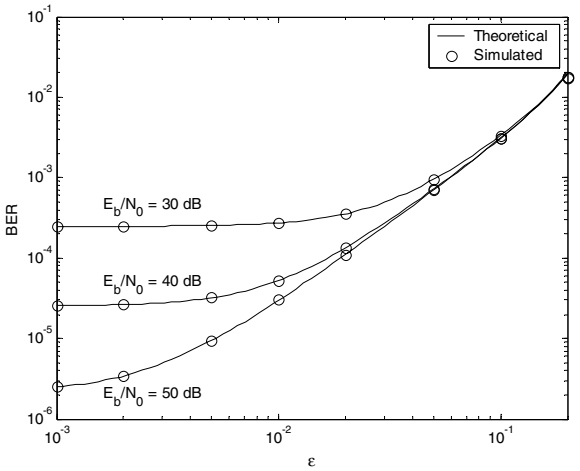

Figure 3. BER of QPSK in the Rayleigh channel B.

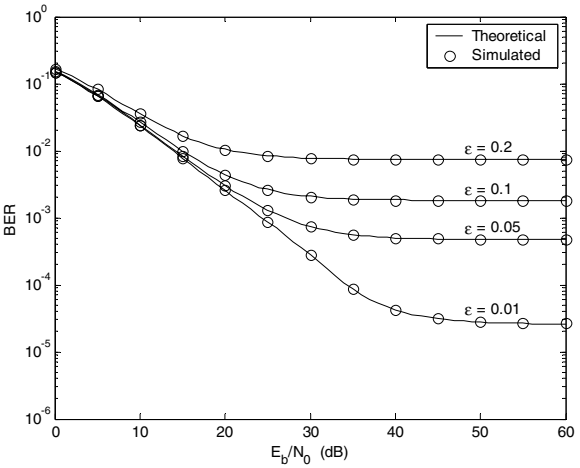

Figure 4. BER of QPSK in the presence of guard bands.

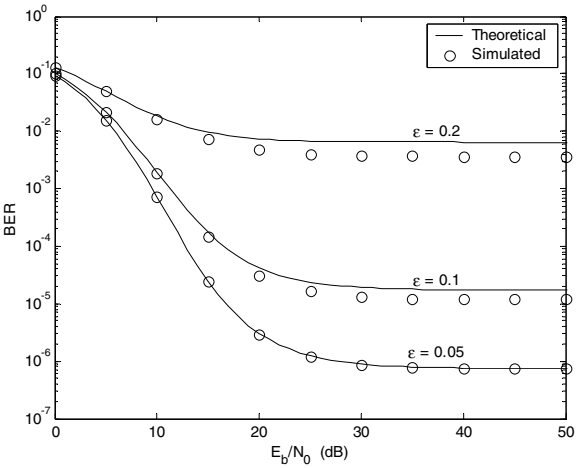

Figure 5. BER of QPSK in the Rician channel D.

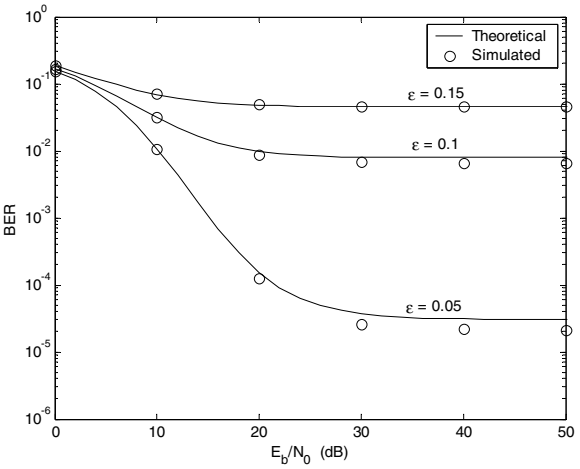

Figure 6. BER of 16-QAM in the Rician channel D.